Regiospecific templated synthesis of D_{2h}-symmetrical tetrakis-adduct $C_{64}(COOEt)_8$ by reversible tether-directed remote functionalization of C_{60}

Francesca Cardullo,[a] Lyle Isaacs,[a] François Diederich,*[a] Jean-Paul Gisselbrecht,[b] Corinne Boudon[b] and Maurice Gross*[b]

[a] *Laboratorium für Organische Chemie, ETH-Zentrum, Universitätstrasse 16, CH-8092 Zürich, Switzerland*
[b] *Laboratoire d'Electrochimie et de Chimie Physique du Corps Solide, U.R.A. au C.N.R.S. No. 405, Faculté de Chimie, Université Louis Pasteur, 1 et 4, rue Blaise Pascal, F-67008 Strasbourg Cedex, France*

Tether-directed remote functionalization of C_{60}, followed by a further addition step and subsequent removal of the tether-reactive group conjugate (template), led to the first D_{2h}-symmetrical tetrakis-adduct in a regiospecific manner.

Regiospecific formation of multiply and differentially functionalized C_{60} derivatives has become a central topic in covalent fullerene chemistry.[1] Polyadducts of C_{60} with well defined three-dimensional structures may provide tailor-made modules for biological and materials applications. In addition, their study helps clarifying the changes in chemical reactivity and physical properties which occur when the conjugated fullerene π-chromophore is reduced in a specific way as a result of increasing functionalization.[2] With the tether-directed remote functionalization, we recently introduced a methodology[3] which allows the regiospecific synthesis of fullerene multiple adducts, such as the C_{2v}-symmetrical tris-adduct **1** (Scheme 1), which are not available otherwise.[1d] Further cyclopropanation of **1** regiospecifically gave the C_s-symmetrical tetrakis-adduct **2** displaying an addition pattern which is also accessible by stepwise tetrakis-cyclopropanation of C_{60}.[4]

In this paper we report a novel C_{60} multiple addition pattern realized for the first time in the synthesis of tetrakis-adducts **3** and **4**. The specific functionalization pattern of **3** and **4**, which

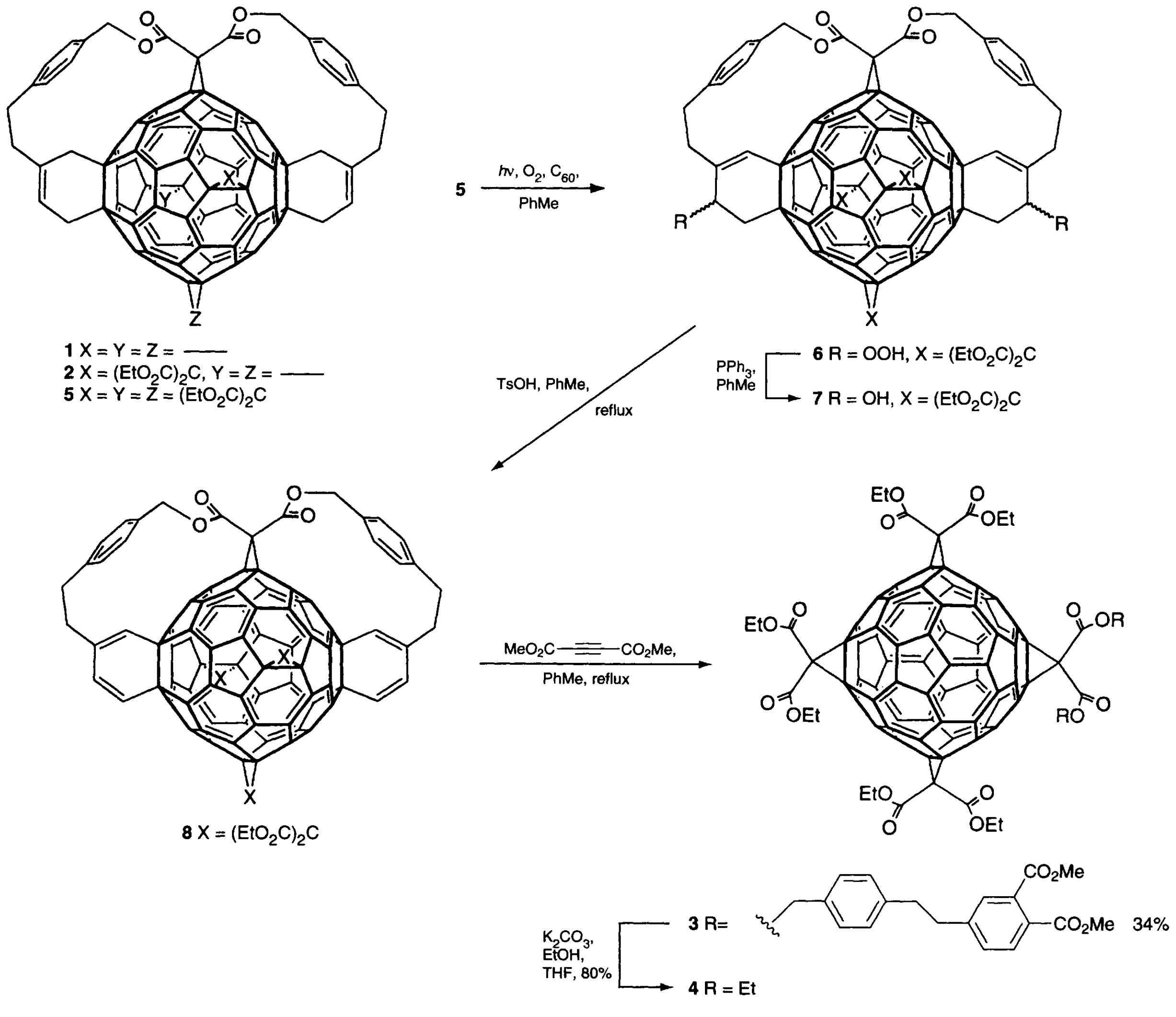

Scheme 1 Synthesis of tetrakis-adducts **3** and **4**. For **6** and **7**, only the constitutional isomer inducing the least amount of strain in the tethers is depicted.

is not accessible by direct addition steps, was achieved by a further development of our tether–remote functionalization method which now permits us to remove the initially introduced tether-reactive group conjugate. In tetrakis-adducts **3** and **4**, all four methano bridges lie on an equatorial belt and the array of cyclopropane rings divides the fullerene core into two equivalent tetrabenzopyracylene substructures linked together by four biphenyl-type bonds (Fig. 1).

The removal of the two cyclohexene rings in hexakis-adduct **5**, which was prepared by threefold addition of diethyl 2-bromomalonate to **1**,[1d] followed an elegant procedure published recently by Rubin and co-workers[5] (Scheme 1). A toluene solution of **5** containing C_{60} as $^1O_2$ sensitizer[6] was irradiated (medium-pressure Hg lamp, Pyrex filter, 25 °C) while a stream of O_2 was bubbled through. The $^1O_2$ ene-reaction at the two cyclohexene rings was completed within 5 hours yielding a mixture of isomeric allylic hydroperoxides **6** with endocyclic[7] double bonds. Reduction of the crude mixture **6** with triphenylphosphane (10 equiv.) gave an isomeric mixture of allylic alcohols **7** which was transformed into the bis(cyclohexadieno) derivative **8** by acid-catalysed dehydration. Addition of dimethyl acetylenedicarboxylate (20 equiv.) to **8** afforded, *via* a Diels–Alder retro-Diels–Alder sequence, C_{2v}-symmetrical tetrakis-adduct **3** in 34% overall yield starting from **5**. Treatment of **3** with K_2CO_3 in THF–EtOH[8] gave the D_{2h}-symmetrical tetrakis-adduct **4** in 80% yield.

Formation of tetrakis-adduct **3** was readily detected by ^1H NMR spectroscopy† which showed two singlets for the methoxy groups and three sets of signals for the dimethyl phthalate ring protons. Furthermore, there are resonances for three chemically nonequivalent ethoxy groups which support the C_{2v}-symmetrical structure. The ^{13}C NMR spectrum† of **3** exhibited 16 of the 17 expected resonances for the fullerene C-atoms and three non-equivalent ethoxycarbonyl groups. The laser desorption-ionization time-of-flight mass spectrum (LDI-TOF MS)† showed the expected molecular ion as the base peak at m/z = 1916. The D_{2h}-symmetrical structure **4** is supported by its ^1H NMR spectrum† which displayed only peaks for the two chemically non-equivalent ethoxy groups. The ^{13}C NMR spectrum† of **4** also confirmed the assigned molecular symmetry by showing seven resonances for fullerene sp^2 C-atoms, one of half intensity, in addition to two signals for fullerene sp^3 C-atoms, two for methano bridge C-atoms, and the expected peaks for two non-equivalent ethoxycarbonyl groups. The LDI-TOF MS† gave the expected molecular ion as the base peak at m/z = 1353.

Tetrakis-adducts **3** and **4** are green–yellow in CH_2Cl_2 solution and their UV–VIS spectra† resemble each other closely (Fig. 2). Despite the four methano bridges at the equator of the molecules, both compounds still possess an extended conjugated π-electron system, consisting of two formal tetrabenzopyracylene substructures connected by four biphenyl-type bonds (Fig. 1). Correspondingly, their end absorptions extend to 650 nm, although the longest wavelength bands are very weak. The electronic absorption spectra of tetrakis-adducts C_{2v}-**3** and D_{2h}-**4** differ significantly from those of the orange–brown C_{2v}-symmetrical tris-adduct **1**, the red C_s-symmetrical tetrakis-adduct **2** (Fig. 2) and the orange-coloured C_s-symmetrical isomer of D_{2h}-**4** with the same addition pattern as in **2**, which was reported by Hirsch *et al.*[4]

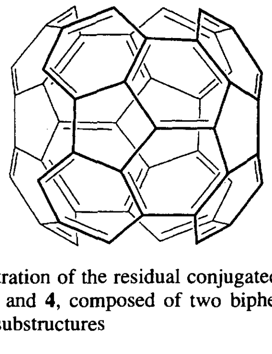

Fig. 1 Schematic illustration of the residual conjugated π-chromophore in C_{60} tetrakis-adducts **3** and **4**, composed of two biphenyl-type connected tetrabenzopyracylene substructures

The electrochemical investigation, carried out as described previously,[2] of tetrakis-adduct **4** afforded three reduction and one oxidation steps in CH_2Cl_2 + 0.1 mol dm^{-3} Bu_4NPF_6 over the available potential range (Tables 1 and 2). By both cyclic and stationary voltammetry, the first two reductions as well as the oxidation step are reversible one-electron charge transfers (Fig. 3).

The reduction potentials of **4** differ strongly from those reported for tetrakis-adduct **2** (Table 1). The two reversible one-electron reductions of **4** occur at a much less negative potential than the corresponding electron transfers in **2**. This could be due to differences in the functional groups in the two tetrakis-adducts, although previous work has shown that the carbon sphere-centred reductions are little affected by the nature of the addends.[2,9] Rather, the conjugated π-chromophore in tetrakis-adduct **4**, with its two biphenyl-type connected tetrabenzopyracylene moieties (Fig. 1) seems to stabilize a mono- and dianion much better than the π-chromophore in tetrakis-adduct **2** with an isomeric, significantly different addition pattern. The specific functionalization seen in **2** (Scheme 1) generates two

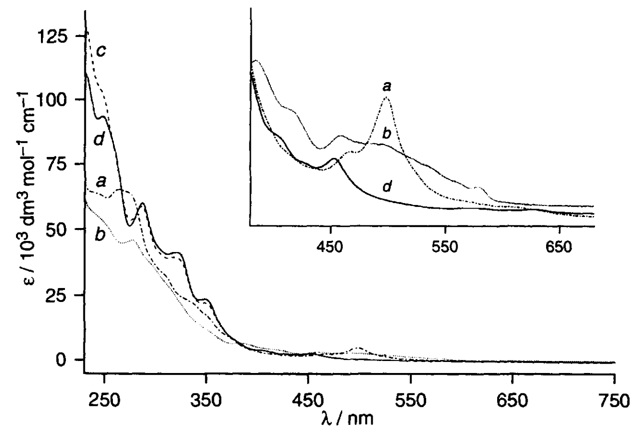

Fig. 2 Electronic absorption spectra of (*a*) **1**, (*b*) **2**, (*c*) **3** and (*d*) **4** in CH_2Cl_2 at c ≈ 10^{-5} mol dm^{-3}. The insert shows the 380–680 nm region in the spectra of **1**, **2** and **4** (recorded at c = 5 × 10^{-4} mol dm^{-3}).

Table 1 Cyclic voltammetry characteristics (*vs.* Fc/Fc+) of multiple adducts **1**, **2**, **4** and **9** on a glassy carbon electrode in CH_2Cl_2 + 0.1 mol dm^{-3} Bu_4NPF_6

	Reduction[a]			Oxidation[a]
Adduct	E_1	E_2	E_3	E_1
4	−1.19 (75)	−1.54 (72)	−2.25[b]	+0.98 (75)
9	−1.18 (75)	−1.56 (75)	−2.20[b]	+1.04 (120)
1	−1.29 (78)	−1.67 (84)	−2.33[b]	+0.90 (92)
2	−1.53 (90)	−1.63 (70)		+0.98 (170)

[a] Values quoted: (E_pa + E_pc)/2 in V and, in parentheses, ΔE_p in mV at 0.1 V s^{-1}. [b] Irreversible process. Value quoted: E_pc in V.

Table 2 Rotating disk electrode characteristics (*vs.* Fc/Fc+) of multiple adduct **4** on a glassy carbon electrode in CH_2Cl_2 + 0.1 mol dm^{-3} Bu_4NPF_6

	Reduction[a]		Oxidation[a]
Adduct	E_1	E_2	E_1
4	−1.19 (64)	−1.55 (59)	+0.98 (62)

[a] Values quoted: $E_{1/2}$ in V and, in parentheses, the slope log $[I(I_d - I)]$ *vs.* E in mV.

benzenoid rings with rather localized electronic sextets, and the corresponding reduction in size of the delocalized fullerene π-chromophore makes it more difficult to accept electrons in the electrochemical reduction. We suggest that the two first, reversibly transferred electrons in **4** are each predominantly delocalized in one of the tetrabenzopyracylene sub-units on opposite sites of the sphere; this proposal is currently being evaluated in computational studies. Interestingly, the reduction potentials measured for tetrakis-adduct **4** resemble more closely those reported for the C_{2v}-symmetrical tris-adduct **1** and the C_s-symmetrical bis-adduct **9** than those reported for tetrakis-adduct **2** (Table 1).[2]

We are now testing whether the previously encountered correlation[2] between the electrophilicity of fullerene derivatives and the ease of electrochemical reduction also holds for **4**, which is expected to exhibit a reactivity toward nucleophiles that is higher than that of tetrakis-adduct **2**, but similar to that of the lower adducts **1** and **9**. The surprising electrochemical results obtained for **4** strongly validate the research concept that characteristic physical and reactivity properties of fullerenes and their covalent derivatives are best explored in correlated studies of multiple adducts with a variety of different functionalization patterns.

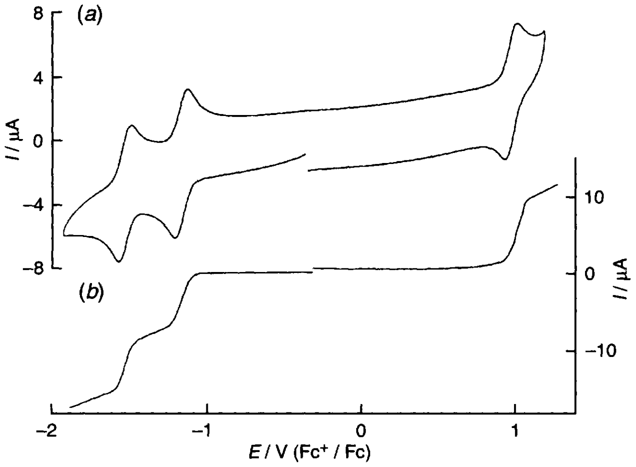

Fig. 3 Electrochemical behaviour of tetrakis-adduct **4** (c = 2 × 10^{-4} mol dm^{-3}) in CH_2Cl_2 + 0.1 mol dm^{-3} Bu_4NPF_6. (*a*) Cyclic voltammetry. Scan rate: 0.1 V s^{-1}. (*b*) Stationary voltammetry on a rotating disk electrode (RDE, N = 2000 rpm). Working electrode: glassy carbon (2 mm diameter). Reference electrode: Ag/AgCl. The ferrocene/ferricinium couple was used as internal standard.

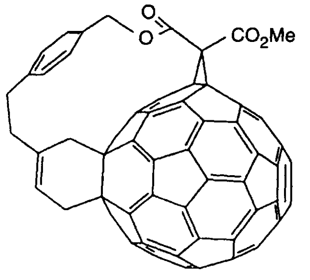

9

Support from the Swiss National Science Foundation is gratefully acknowledged.

Footnote

† *Spectroscopic data* for **3**: UV–VIS (CH_2Cl_2) λ_{max}/nm 453 (ε dm^3 mol^{-1} cm^{-1} 2700), 405sh (4050), 346sh (22400), 318 (39700), 286 (59100) and 245sh (104100); ^{1}H NMR (500 MHz, $CDCl_3$) δ 1.43 (t, *J* 7.1, 6 H), 1.44 (t, *J* 7.1, 6 H), 1.45 (t, *J* 7.1, 6 H), 2.83–3.95 (m, 8 H), 3.88 (s, 6 H), 3.90 (s, 6 H), 4.49 (q, *J* 7.1, 4 H), 4.51 (q, *J* 7.1, 4 H), 4.52 (q, *J* 7.1, 4 H), 5.37 (s, 4 H), 7.11 (d, *J* 8.1, 4 H), 7.26 (dd, *J* 7.9 and 1.8, 2 H), 7.30 (d, *J* 8.1, 4 H), 7.49 (d, *J* 1.8, 2 H) and 7.65 (d, *J* 7.9, 2 H); ^{13}C NMR (125 MHz, $CDCl_3$) δ 14.06, 14.13, 14.15, 36.95, 37.36, 43.91, 44.29, 46.84, 52.47, 52.60, 63.12, 63.14, 63.18, 68.52, 69.86, 69.97, 71.16, 128.55, 128.60, 129.12, 129.20, 129.26, 130.87, 132.62, 132.68, 140.77, 140.83, 141.43, 141.89, 142.20, 142.41, 142.42, 142.52, 142.65, 144.22, 144.24, 144.32, 145.37, 145.40, 145.41, 163.68, 163.82, 164.07, 164.12, 167.65 and 168.39; LDI-TOF-MS: *m*/*z* 1916 [M$^-$]. For **4**: UV–VIS (CH_2Cl_2) λ_{max}/nm 626 (ε/dm^3 mol^{-1} cm^{-1} = 200), 573 (250), 453 (2850), 409sh (3750), 348sh (23700), 320 (41700), 287 (60400) and 245 (93600); ^{1}H NMR (500 MHz, $CDCl_3$) δ 1.44 (t, *J* 7.1, 12 H), 1.46 (t, *J* 7.1, 12 H), 4.50 (q, *J* 7.1, 8 H) and 4.52 (q, *J* 7.1, 8 H); ^{13}C NMR (125 MHz, $CDCl_3$) δ 14.14, 14.16, 44.28, 46.83, 63.12, 63.17, 69.98, 71.17, 140.87, 142.20, 142.45, 142.64, 144.24, 144.35, 145.44, 163.86 and 164.15. LDI-TOF-MS: *m*/*z* 1353 [M$^-$].

References

1 (*a*) A. Hirsch, *The Chemistry of the Fullerenes*, Georg Thieme, Stuttgart, 1994; (*b*) F. Diederich and C. Thilgen, *Science*, 1996, **271**, 317; (*c*) H. W. Kroto, R. Taylor and D. R. M. Walton, *Pure Appl. Chem.*, 1994, **66**, 2091; (*d*) L. Isaacs, R. F. Haldimann and F. Diederich, *Angew. Chem.*, 1994, **106**, 2434; *Angew. Chem., Int. Ed. Engl.*, 1994, **33**, 2339; (*e*) L. Isaacs, P. Seiler and F. Diederich, *Angew. Chem.*, 1995, **107**, 1636; *Angew. Chem. Int. Ed. Engl.*, 1995, **34**, 1466; (*f*) I. Lamparth, C. Maichle-Mössmer and A. Hirsch, *Angew. Chem.*, 1995, **107**, 1755; *Angew. Chem., Int. Ed. Engl.*, 1995, **34**, 1607; (*g*) B. Kräutler and J. Maynollo, *Angew. Chem.*, 1995, **107**, 69; *Angew. Chem. Int. Ed. Engl.*, 1995, **34**, 87; (*h*) P. J. Fagan, J. C. Calabrese and B. Malone, *J. Am. Chem. Soc.*, 1991, **113**, 9408.
2 C. Boudon, J.-P. Gisselbrecht, M. Gross, L. Isaacs, H. L. Anderson, R. Faust and F. Diederich, *Helv. Chim. Acta*, 1995, **78**, 1334.
3 R. Breslow, *Acc. Chem. Res.*, 1980, **13**, 170.
4 A. Hirsch, I. Lamparth and T. Grösser, *J. Am. Chem. Soc.*, 1994, **116**, 9385.
5 Y.-Z. An, G. A. Ellis, A. L. Viado and Y. Rubin, *J. Org. Chem.*, 1995, **60**, 6353.
6 J. W. Arbogast, A. P. Darmanyan, C. S. Foote, Y. Rubin, F. Diederich, M. M. Alvarez, S. J. Anz and R. L. Whetten, *J. Phys. Chem.*, 1991, **95**, 11.
7 Y.-Z. An and Y. Rubin, *Abstracts of Papers, 209th National Meeting of the American Chemical Society*, Anaheim, CA, American Chemical Society, Washington, D.C., 1995; Abstract OCGN 66.
8 F. Diederich and J.-F. Nierengarten, unpublished results.
9 T. Suzuki, Q. Li, K. C. Khemani, F. Wudl and Ö. Almarsson, *J. Am. Chem. Soc.*, 1992, **114**, 7300; T. Suzuki, Y. Maruyama, T. Akasaka, W. Ando, K. Kobayashi and S. Nagase, *J. Am. Chem. Soc.*, 1994, **116**, 1359; F. Arias, Q. Xie, Y. Wu, Q. Lu, S. R. Wilson and L. Echegoyen, *J. Am. Chem. Soc.*, 1994, **116**, 6388.

Received, 14th December 1995; Com. 5/08140H